Reactions of Dicobalt Octacarbonyl with Dinucleating and Mononucleating Bis(imino)pyridine Ligands

Journal:	*Dalton Transactions*
Manuscript ID	DT-ART-08-2018-003405.R2
Article Type:	Paper
Date Submitted by the Author:	25-Sep-2018
Complete List of Authors:	Groysman, Stanislav; Wayne State University, Chemistry Hollingsworth, Ryan; Wayne State University, Chemistry Lord, Richard; Grand Valley State University, Chemistry Martin, Philip; Wayne State University, Chemistry Grass, Amanda; Wayne State University, Chemistry Beattie, Jeffrey; Wayne State University, Chemistry

SCHOLARONE™
Manuscripts

Reactions of Dicobalt Octacarbonyl with Dinucleating and Mononucleating Bis(imino)pyridine Ligands

Ryan L. Hollingsworth,[a] Jeffrey W. Beattie,[a] Amanda Grass,[a] Philip D. Martin,[b] Stanislav Groysman*[a], and Richard L. Lord*[c]

[a]Department of Chemistry, Wayne State University, 5101 Cass Ave, Detroit, MI, 48202, USA. E-mail: groysman@chem.wayne.edu

[b]Lumigen Instrument Center, Wayne State University, 5101 Cass Ave, Detroit, MI, 48202, USA.

[c]Department of Chemistry, Grand Valley State University, Allendale, MI, 49401, USA. E-mail: lordri@gvsu.edu

Abstract

This work focuses on the application of dicobalt octacarbonyl ($Co_2(CO)_8$) as a metal precursor in the chemistry of formally low-valent cobalt with redox-active bis(imino)pyridine [NNN] ligands. The reactions of both mononucleating mesityl-substituted bis(aldimino)pyridine (L^1) and dinucleating macrocyclic xanthene-bridged di(bis(aldimino)pyridine) (L^2) with $Co_2(CO)_8$ were investigated. Independent of the metal-to-ligand ratio (1:1 or 1:2 ligand to $Co_2(CO)_8$), the reaction of the dinucleating ligand L^2 with $Co_2(CO)_8$ produces a tetranuclear complex $[Co_4(L^2)(CO)_{10}]$ featuring two discrete $[Co_2[NNN](CO)_5]$ units. In contrast, a related mononucleating bis(aldimino)pyridine ligand, L^1, produces different species at different ligand to $Co_2(CO)_8$ ratios, including dinuclear $[Co_2(CO)_5(L^1)]$ and zwitterionic $[Co(L^1)_2][Co(CO)_4]$. Interestingly, $[Co_4(L^2)(CO)_{10}]$ features metal-metal bonds, and no bridging carbonyls, whereas $[Co_2(CO)_5(L^1)]$ contains cobalt centers bridged by one or two carbonyl ligands. In either case, treatment with excess acetonitrile leads to disproportionation to the zwitterionic $[Co[NNN](NCMe)_2][Co(CO)_4]$ units. The electronic structures of the complexes described above were studied with density functional theory. All the obtained bis(imino)pyridine complexes serve as catalysts for cyclotrimerization of methyl propiolate, albeit their reactivity is inferior compared with $Co_2(CO)_8$.

Introduction

The past decade has witnessed growing interest in the design of bimetallic complexes due to the anticipated cooperativity between two nearby metal centers.[1-3] One particularly fascinating subfield of this research area involves redox-active dinucleating ligands, which allow for the combination of metal-metal and metal-ligand cooperativity.[4] Catalytically competent complexes of redox-active ligands generally require metals in formally low oxidation states.[5-8] Such complexes can be obtained by a "two-step" protocol, which involves first synthesis of the oxidized metal complexes (i.e. Ni(II) or Co(II)) then a reduction.[9] For example, Chirik described synthesis of $[NNN]Fe(N_2)_2$ and $[NNN]Fe(CO)_2$ complexes ([NNN] = redox-active pyridinediimine alternatively termed bis(imino)pyridine) by the reduction of $[NNN]FeX_2$ precursors.[10] Alternatively, formally reduced monometallic/bimetallic metal complexes with redox-active ligands can be obtained in a single step, if a reduced metal precursor is available. While low-boiling $Ni(CO)_4$[11] is generally considered too toxic for contemporary laboratory synthesis, formally Ni(0) complexes with dinucleating and mononucleating redox-active ligands can be conveniently obtained by the direct reaction of $Ni(COD)_2$ with a variety of redox-active ligand precursors.[12] Dicobalt octacarbonyl $Co_2(CO)_8$ is one of the most decorated organometallic complexes, whose original synthesis by Mond and coworkers was published in 1910.[13] As $Co_2(CO)_8$ is a solid, it does not constitute as acute of an inhalation hazard as $Ni(CO)_4$. As a result, $Co_2(CO)_8$ is frequently utilized as a pre-catalyst in organometallic chemistry,[14] in the synthesis of nanomaterials,[15] metal clusters, and extended solids.[16] $Co_2(CO)_8$ also appears to be a viable candidate as a metal precursor for the synthesis of the formally reduced dinuclear or cobalt complexes with redox-active ligands, both mononucleating and dinucleating. Yet, the reports of its use with such ligands are relatively scarce, and generally require benzoquinone or closely related amidophenolate as a co-reactant.[17] Wender, Sternberg and Orchin explored the reactivity of phenanthroline with $Co_2(CO)_8$,[18] that resulted in the disproportionation of Co(0) into a Co(II) cation and two Co(1-) anions. More recently, Weighardt and coworkers explored the reactivity of $Co_2(CO)_8$ with terpyridine.[19] Chirik and coworkers prepared a bis(imino)pyridine cobalt carbonyl complex, but this complex was obtained indirectly using cobalt-dinitrogen precursor.[20] We, and others, have previously shown that formally Ni(0) source, $Ni(COD)_2$, is a highly useful precursor in the chemistry of low-valent nickel with redox-active mononucleating

and dinucleating ligands featuring iminopyridine and bis(imino)pyridine chelates.[12] Motivated by these findings, we became interested in the exploration of the chemistry of $Co_2(CO)_8$ with bis(imino)pyridine ligands. Herein we report synthetic, structural, and density functional theory (DFT) study on the reactivity of $Co_2(CO)_8$ with dinucleating and mononucleating bis(imino)pyridine ligands.

Results and discussion

Synthesis and characterization of the macrocyclic ligand precursor L^2

This study focuses on the reactivity of new dinucleating macrocyclic xanthene-bridged di(bis(imino)pyridine) L^2 and previously reported bis(imino)pyridine L^1.[12f] Macrocycle L^2 is synthesized by the acid-catalyzed condensation of the corresponding dialdehyde with xanthene diamine linker (**Scheme 1**). 2,6-Pyridinedicarboxaldehyde is added to a methanol solution of the xanthene linker (2,7-di-*tert*-butyl-9,9-dimethyl-9*H*-xanthene-4,5-diamine),[21] with a catalytic amount of acetic acid, and refluxed for 24 hours. The product precipitates as a pale yellow solid, and is isolated in 85% yield. We note that no template is required for the synthesis of this rigid xanthene-linked macrocycle, unlike our previously reported *para*-xylylene di(bis(imino)pyridine) macrocycle.[22] The ligand is characterized by ^{1}H and ^{13}C{^{1}H} NMR spectroscopy and high-resolution mass spectrometry (HRMS). NMR spectra demonstrate effective C_{2v} symmetry in solution, consistent with the rigid "bowl" structures observed for all complexes. Thus, four *tert*-butyl groups give rise to a single peak. In contrast, two different signals are observed for the methyl groups, indicating the lack of exchange between the "inner" and the "outer" methyls (Me$_{in}$ and Me$_{out}$, see **Scheme 1**). We note that a related ligand with methyl groups in the imine positions has been previously synthesized.[23]
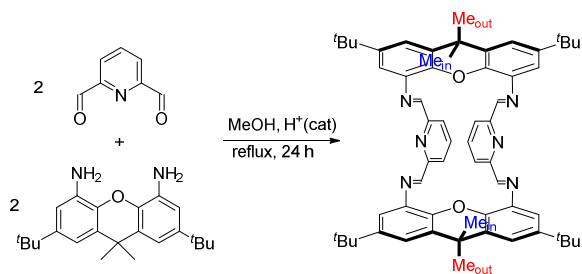
Scheme 1. Synthesis of L^2.

Synthesis and structures of the products of the reactions of L^2/L^1 with $Co_2(CO)_8$

As mentioned earlier, this work focuses on the reactivity of $Co_2(CO)_8$ as a precursor for the chemistry of formally low-valent cobalt with redox-active bis(imino)pyridine ligands. To obtain a dinuclear complex of L^2, it was treated with one equivalent of $Co_2(CO)_8$ at room temperature for 24 hours (**Scheme 2**). In contrast to our expectations, this reaction produced tetranuclear complex $[Co_4(L^2)(CO)_{10}]$ (**1**), that is isolated as red-violet crystals by recrystallization from diethyl ether in 37% yield (with respect to the ligand). The yield of the tetranuclear complex can be improved by using 1:2 ratio of L^2 with $Co_2(CO)_8$. Overnight recrystallization in diethyl ether produced dark red crystals of **1** in 96% yield.
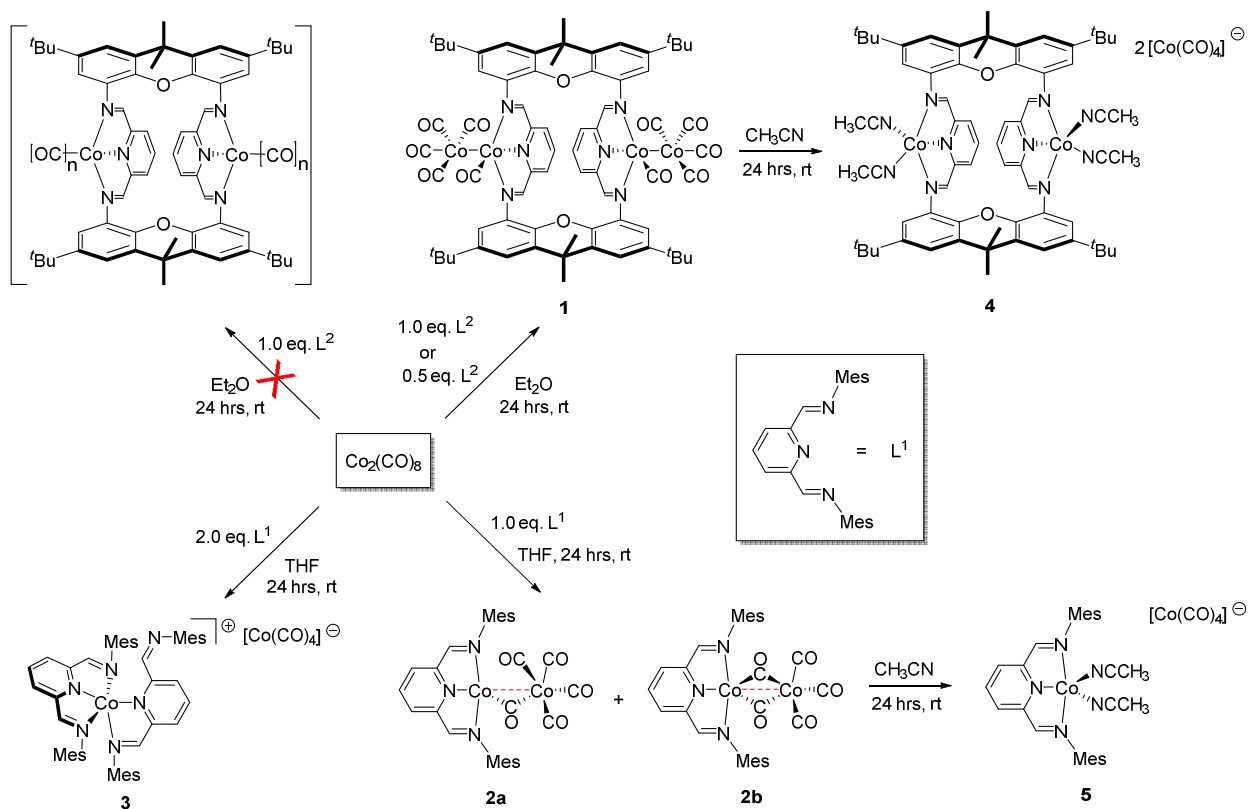
Scheme 2. Reactivity of L^1 and L^2 with $Co_2(CO)_8$. For the structure of L^2, see Scheme 1

Complex **1** was characterized by NMR spectroscopy, IR spectroscopy, X-ray crystallography, and elemental analysis. ^1H NMR spectrum of **1** suggests a single species of approximate C_{2v} symmetry in solution, based on one signal for all *tert*-butyl groups and two

signals for the xanthene methyl groups. ^{13}C spectrum is consistent with a single species of C_{2v} symmetry in solution, demonstrating the expected five signals in the aliphatic region and ten signals in the aromatic/imino region (see ESI). However, two signals are observed for CO carbons (210.75 and 203.81 ppm), indicating that more than one type of CO ligand is present. The X-ray structure determination confirms a tetranuclear complex of $[Co_4(L^2)(CO)_{10}]$ composition. Intriguingly, **1** crystallizes in two slightly different forms (**1** as red plates and **1'** as red needles) that are two conformational isomers (**Figure 1**), suggesting some conformational flexibility of the macrocycle. Both structures demonstrate two discrete identical (crystallographic C_2 symmetry in both structures) bimetallic "[NNN]Co(CO)Co(CO)$_4$" fragments. Each "[NNN]Co(CO)Co(CO)$_4$" fragment is held together by a metal-metal bond; no bridging carbonyls are observed. Co-Co bond distances within these bimetallic units (2.80(1) Å) are slightly longer than the Co-Co bond distance in the minor structural isomer of $Co_2(CO)_8$ that exhibits no bridging carbonyls (2.70 Å).[24] No interaction is observed between two internal cobalts (Co2 --- Co2' distances of 4.8 and 5.2 Å). The redox-active nature of the [NNN] chelates is confirmed by the changes in the imino C=N and C-C bonds (Table 1)[10, 12, 20] and by DFT calculations (see below). As the structure of **1'** is of relatively low quality, only detailed structural parameters of **1** are presented in Table 1; however, metrics of **1'** are similar to **1**. The structure demonstrates electron delocalization along the redox-active chelates, with elongated C_{im}-N_{im} bond lengths of 1.330(4) and 1.314(4) Å and condensed C_{im}-C_{py} bond lengths of 1.426(4)/1.437(4) Å. Using the previously described τ parameter,[25] the geometry at both internal and lateral cobalts in **1** is best described as distorted square pyramidal.
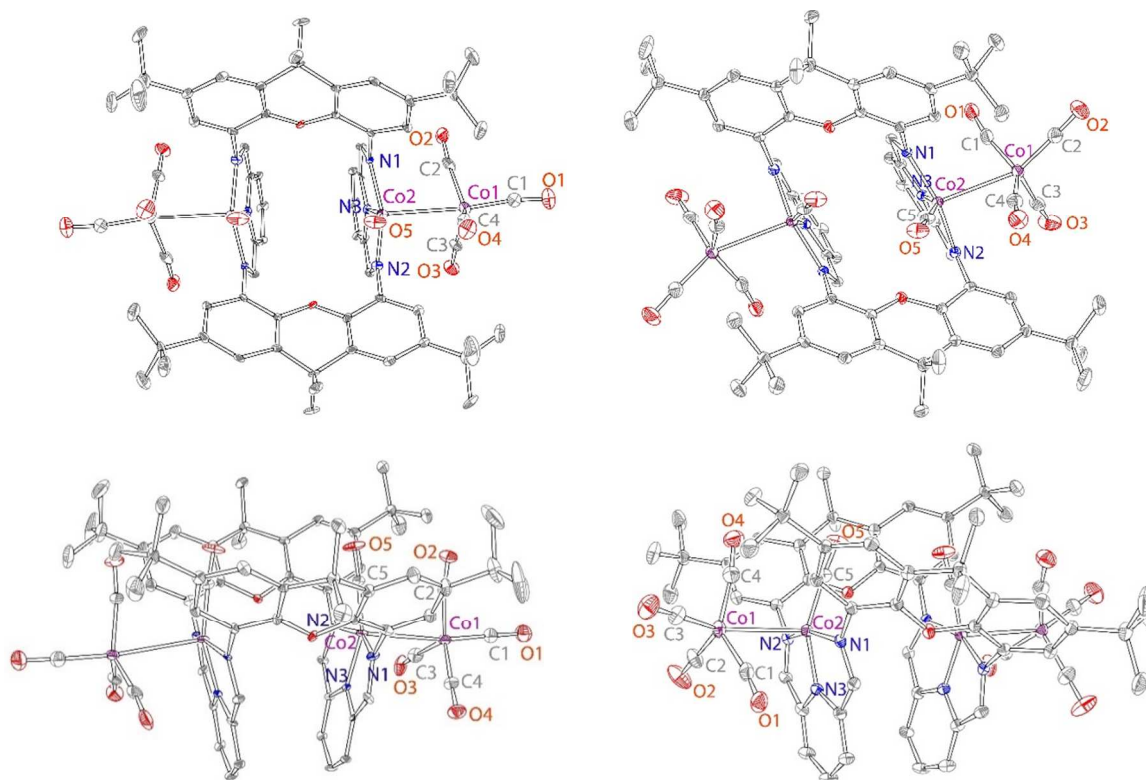
Figure 1: X-ray crystal structures of **1'** (left – top and side view) and **1** (right – top and side view), 50% probability ellipsoids. H atoms and co-crystallized solvents are omitted for clarity. Selected bond distances (Å) and angles (°) for **1**: Co2-Co1 2.798(1), Co2---Co2' 4.815(1), Co1-N1 1.920(3), Co1-N2 1.924(2), Co2-N3 1.833(3), Co1-C2 1.754(4), Co1-C1 1.773(4), Co1-C3 1.778(4), Co1-C4 1.784(4), Co2-C5 1.774(4), Co2-Co1-C2 150.2(1), C4-Co1-C1 137.1(2).

Table 1. Selected bond lengths for **1**, **3**, and **4**.[a]

	$C_{im}=N_{im}$	$C_{im}-C_{py}$
1[b]	1.330(4)/1.314(4)	1.437(4)/1.426(4)
3	1.312(4)/1.309(4)[c]	1.414(4)/1.415(4)[c]
	1.288(4)/1.262(4)[d]	1.456(4)/ 1.475(4)[d]
4	1.305(4)/1.326(4)	1.420(4)/1.424(4)
	1.319(4)/1.321(4)	1.420(4)/1.423(4)

[a]Due to relatively low C-C bond precision of structure **2**, its metrics are not discussed. [b]Due to crystallographic C_2 symmetry of **1**, two different bond distances were observed. [c]Bond distances in fully bound bis(imino)pyridine in **3**. [d]Bond distances in bis(imino)pyridine bound through a single iminopyridine.

The observed formation of complex **1** stands in sharp contrast to the anticipated di-cobalt complex, where each cobalt liberates two/three CO molecules to form hypothetical

"[Co$_2$(L^2)(CO)$_{2/3/4}$]" species (Scheme 2). We note that the reactions of Co$_2$(CO)$_8$ are strongly substrate-dependent, and may lead to either partial or full substitution of carbonyl ligands. In some cases, retention of the significant number of the carbonyl ligands and the overall dinuclear structure is observed (e. g [(CHD)$_2$Co$_2$(CO)$_4$] or [(NHC)$_2$Co$_2$(CO)$_6$] (CHD = 1,3-cyclohexadiene, NHC = N-heterocyclic carbene) or (**Figure 2, A** and **B**).[26, 27] Along the same lines, Agapie and coworkers have recently reported that a dinucleating arene-bridged diphosphine forms complex **C** in the reaction with Co$_2$(CO)$_8$ (**Figure 2, C**).[28] In other cases, full ligand substitution at one of the cobalts leads to the metal-metal bond splitting and formation of ion pairs featuring [Co^{1-}(CO)$_4$]$^-$ as an anion (e.g. [Co^I(terpy)$_2$][Co^{1-}(CO)$_4$], **Figure 2**, **D**; terpy = terpyridine).[18,19,29] Interestingly, relatively small changes on the ligand periphery may have a significant effect on the outcome of the reaction with Co$_2$(CO)$_8$. Thus, Wieghardt and coworkers showed that while the reaction of unsubstituted terpy with Co$_2$(CO)$_8$ forms [Co^I(terpy)$_2$][Co^{1-}(CO)$_4$], the reaction of 4,4',4''-tri-tert-butyl-2,2':6',2''-terpyridine (t-terpy) forms [Co^{II}(t-terpy)$_3$][Co^{1-}(CO)$_4$]$_2$.[19] Others showed that the full release of all CO ligands and splitting of Co-Co interaction is possible in both mononucleating and dinucleating systems.[17] One could hypothesize that the observed formation of a tetranuclear (instead of dinuclear) complex in the present system independent of the L^2-to-Co$_2$CO$_8$ ratio results from the relatively long distance between chelating bis(aldimino)pyridine units in L^2, combined with its relative rigidity and the overall steric bulk. Because of these factors, each chelating unit reacts preferentially with one equivalent of Co$_2$(CO)$_8$. To test this hypothesis, we investigated the reactivity of a mononucleating analogue of L^2, L^1 (**Scheme 2**), with Co$_2$(CO)$_8$. The synthesis and reactivity of L^1 with nickel were previously reported.[12f]
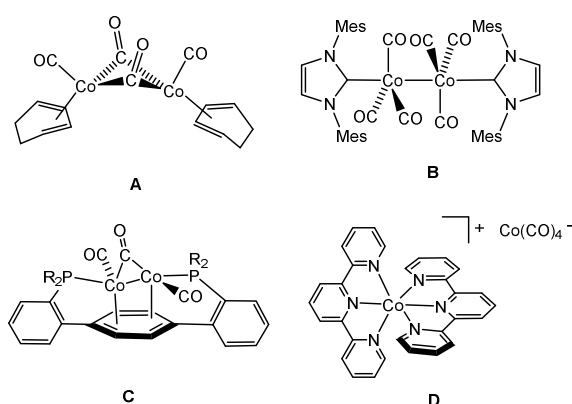

Figure 2. Examples of products of the reactions of Co$_2$(CO)$_8$ with various ligands.[19, 26-28]

Mixing one equivalent of L^1 with $Co_2(CO)_8$ forms a red-purple solution, from which complex **2** is isolated as a purple solid in 88% yield. X-ray quality crystals of **2** are obtained by recrystallization from pentane. Spectral and structural data for **2** are consistent with $[Co_2(L^1)(CO)_5]$ composition, similar to the corresponding complexes of the dinucleating ligand. There are, however, some notable differences between the systems. While NMR spectroscopy for **2** indicates a single species in solution, IR spectroscopy suggests the presence of both terminal and bridging carbonyls (see below for the discussion of IR spectra). We also note the overall similarity between the UV-vis spectra of **2** and **1** (see Figures S12 and S13 in the SI), with the difference being three peaks observed for **1** ($\lambda = 719$, 542, and 487 nm) and four peaks for **2** (767, 711, 556, 495 nm). Consistent with the spectral data, two different structural isomers (**2a** and **2b**) are observed for the solid-state structure of **2**, co-crystallizing in the same unit cell. Isomer **2a** contains square-pyramidal Co1 center ligated by the [NNN] chelate and two carbonyls, and distorted tetrahedral Co2 center ligated by four carbonyls. **2b** contains a square-pyramidal Co3 center, ligated by bis(aldimino)pyridine and two carbonyls, and trigonal bipyramidal Co4 center, displaying five carbonyl ligands. The major difference between the isomers is in the number of bridging carbonyls: one for **2a** and two for **2b**. Accordingly, **2b** manifests a significantly shortened Co--Co distance of 2.594(1) Å, vs. 2.703(1) Å in **2a**. The electronic structure of **2b** was also investigated computationally (vide infra). We note that $Co_2(CO)_8$ is also known to be structurally fluxional, displaying structures with and without bridging carbonyls.[24, 30, 31]
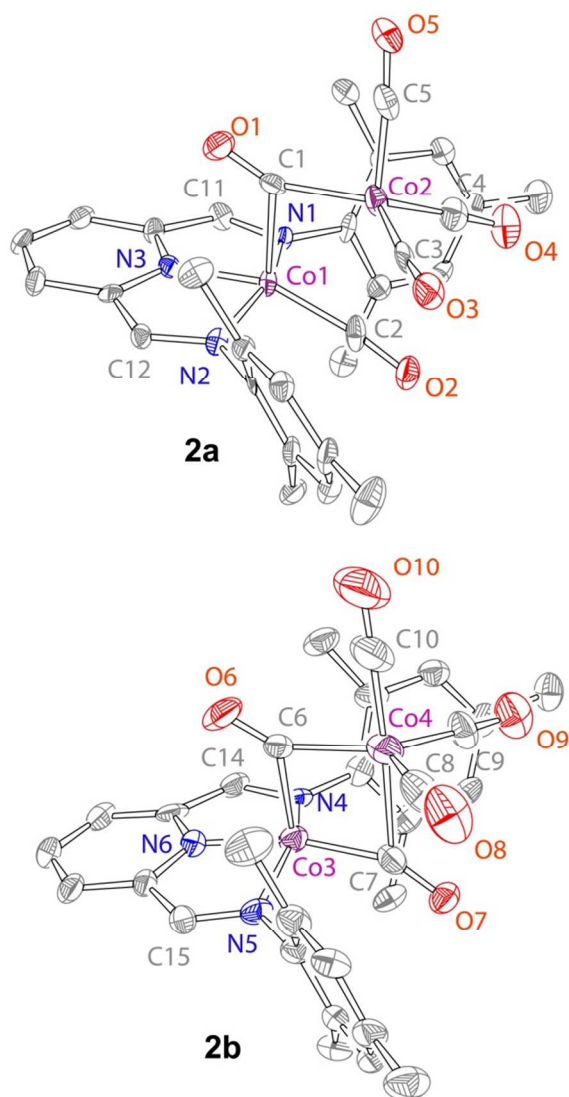
Figure 3. X-ray structure of **2a** and **2b**, 50% probability ellipsoids. Selected bond distances (Å): Co1-Co2 2.703(1), Co1-C1 2.087(6), Co2-C1 1.815(7), Co1-C2 1.783(6), Co2---C2 2.663(6), Co3-Co4 2.594(1), Co3-C6 1.960(6), Co4-C6 1.894(6), Co3-C7 1.814(6), Co4-C7 2.220(6).

Treatment of $Co_2(CO)_8$ with two equivalents of L^1 leads to the formation of purple solutions from which complex **3** is isolated in 57% yield. In a sharp contrast to **1** or **2**, complex **3** is paramagnetic, displaying four broad proton resonances in approximately 20 ppm range. Purple crystals of **3** were obtained from cold saturated THF solution; the structure is given in **Figure 3**

below. Structure determination of **3** reveals a zwitterion pair $[Co(L^1)_2][Co(CO)_4]$. Thus, at 2:1 ratio, mononucleating bis(aldimino)pyridine ligand reacts with $Co_2(CO)_8$ similarly to terpy.[19] Interestingly, in $[Co(terpy)_2][Co(CO)_4]$ the cationic cobalt center exhibited pseudooctahedral coordination, with nearly symmetric binding of terpy ligands. In contrast, $[Co(L^1)_2][Co(CO)_4]$ demonstrates penta-coordinate ($\tau = 0.34$) geometry. One of the [NNN] chelates is bound through all three nitrogens, while the other is bound only through one of the iminopyridines, with the second imine unbound. As expected, while the κ^3-bound [NNN] exhibits full redox delocalization, typical C=N double and C-C single bonds consistent with a neutral chelate are observed for the unbound imine arms. The electronic structure calculations on the cation in **3** are discussed below.
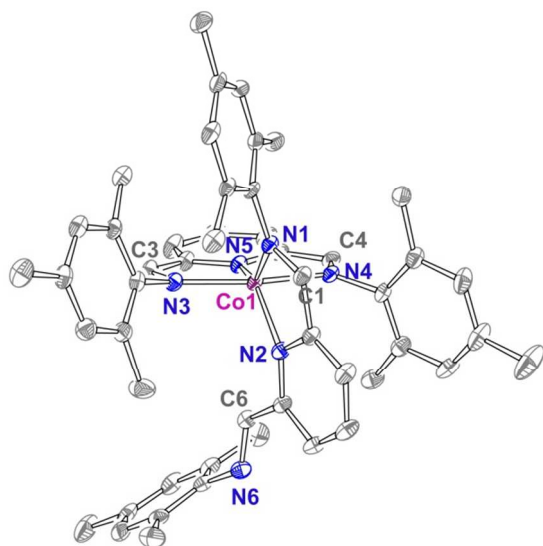

Figure 4. X-ray structure of **3**, 50% probability ellipsoids. H atoms, $[Co(CO)_4]$ anion, and co-crystallized THF are omitted for clarity. Selected bond distances (Å) and angles (°): Co1-N1 2.012, Co1-N2 2.030(2), Co1-N3 1.945(2), Co1-N4 1.978(2), Co1-N5 1.810(2), N3-Co1-N4 161.0(1), N1-Co1-N5 140.8(1), N2-Co1-N5 138.2(1).

The experiments above suggest significant differences between the mononucleating and the dinucleating systems. At 1:2 ratio of chelating [NNN] units to $Co_2(CO)_8$, both dinucleating and mononucleating bis(aldimino)pyridines form non-symmetric species of $[Co_2(L)(CO)_5]$ type. At 1:1 ratio, however, the behavior of the mononucleating ligand L^1 diverges significantly from the behavior of the dinucleating systems, forming $[Co(L^1)_2][Co(CO)_4]$, similar to the previously

reported bipy/terpy chemistry. Thus, we conclude that it is the dinucleating nature of L^2 in the present case that is the responsible for the stability of the tetranuclear complex **1**.

As demonstrated in this work (complex **4**) and elsewhere in the literature, the Co-Co bond in $Co_2(CO)_n(L)_{8-n}$ is capable of undergoing heterolytic bond cleavage upon reaction with various L-type ligands including pyridine, isocyanide, and phosphine.[32] Inspired by the formation of complex **3**, we attempted to split Co-Co bonds in **1** by treating it first with PPh_3. Addition of PPh_3 to **1** (4 equivalents) leads to the formation of a green-brown solution. ^{31}P NMR spectrum contained a new signal around 40 ppm, indicating formation of a new product. ^{1}H NMR, however, suggested formation of a mixture of products, which we were not able to separate. The reactivity of **1** with excess acetonitrile was explored next. Dissolution of dark red-purple **1** in acetonitrile leads to the formation of green solution, from which complex **4** was isolated by recrystallization from acetonitrile/ether mixture. Proton NMR spectrum of complex **4** (taken in CD_3CN) demonstrates the expected five resonances in the aromatic region, two distinct methyl group resonances, and a single resonance for the *tert*-butyl groups. Most significantly, the spectrum contains a signal at 1.96 ppm, whose intergration signifies the presence of four acetonitrile molecules. The X-ray structure of **4** (**Figure 5**) demonstrates di-cationic, formally di-Co(I), complex balanced by two $[Co^{1-}(CO)_4]^-$ anions. As in the other L^2 structures reported in this manuscript (**1a/1b**), the two [NNN] chelates are nearly co-parallel, displaying interplanar angle of 6 degrees. Both cobalt centers are distorted square pyramidal, exhibiting τ values of 0.07 and 0.18. Bis(imino)pyridine metrics (see Table 1) and DFT calculations (below) indicate that [NNN] chelates are reduced, and that Co centers are likely Co(II). Similar chemistry was observed with the mononuclear analogue: dissolution of complex **2** in acetonitrile forms complex **5**. While we were not able to obtain the structure of complex **5**, its NMR and IR characterization suggests $[Co[NNN](NCMe)_2][Co(CO)_4]$ formulation. In addition, the UV-vis spectrum of **5** closely resembles that of **4**. Both compounds display three peaks in the 400-900 nm region featuring similar wavelength and absorptivity values (Figures S15 and S16).
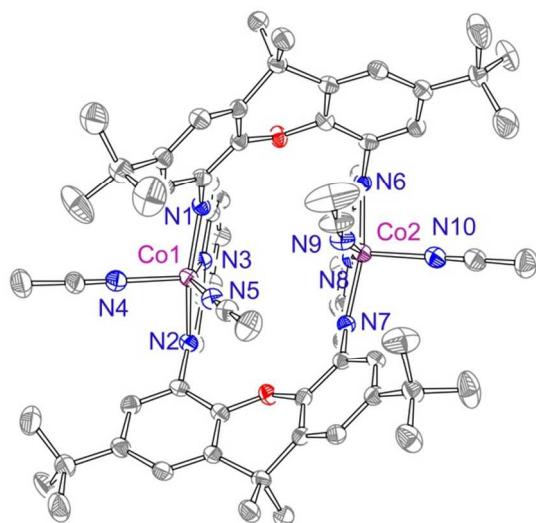
Figure 5. X-ray structure of **4**, 50% probability ellipsoids. H atoms and [Co(CO)$_4$] anions are omitted for clarity. Selected bond distances (Å) and angles (°): Co1-N1 1.934(3), Co1-N2 1.936(3), Co1-N3 1.814, Co1-N4 2.030(3), Co1-N5 1.928(3), N1-Co1-N2 160.0(1), N3-Co1-N5 155.0(1).

IR spectroscopy

The IR spectra for all compounds in the carbonyl region are summarized in **Figure 6**. The comparison between different IR spectra leads to several noteworthy conclusions. First, as anticipated, only compound **2** demonstrates the peak associated with a bridging carbonyl around 1800 cm^{-1} (bridging carbonyls generally occur below 1850 cm^{-1}). The second noteworthy feature is the presence of a strong peak in the 1860-1890 cm^{-1} area in the spectra of all the compounds. The presence of a strong peak in this region is often associated with a $[Co^{1-}(CO)_4]^-$ ion.[33] In contrast, any of the known isomers of $Co_2(CO)_8$ ($C_{2v}/D_{2d}/D_{3d}$), which contain Co(0), do not feature signals in this area.[31] Compounds **3**-**5** contain genuine $[Co^{1-}(CO)_4]^-$ counter-ion, and thus the presence of a single very strong carbonyl resonance around 1870 cm^{-1} is well justified. What explains the presence of the peak around 1880/1890 cm^{-1} in the spectra of compounds **1** and **2**, that contain formally Co(0) oxidation states in the "[Co(CO)$_4$]" units? One possible explanation for this phenomenon is that the redox non-innocence within the "[NNN]Co(CO)" fragment of

dinuclear structures extends to the $[Co(CO)_4]$ to which it is linked, making it effectively $[Co^{1-}(CO)_4]^{-}$, To probe this and other electronic structure questions, we turned to DFT calculations.
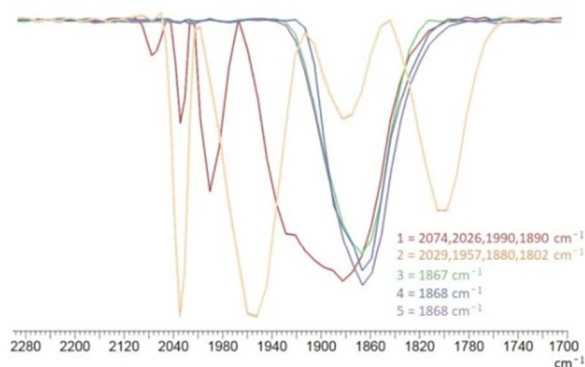

Figure 6. IR spectra of compounds **1-5** in 1700-2300 cm^{-1} range. ATR-FTIR was used to record all IR spectra of powdered samples.

DFT calculations

Calculations at the B3LYP-D3/6-31G(d) level of theory were performed on model complexes of the di- and mono-nucleating ligands.[34] Because L^2 has a ^tBu group meta to the iminopyridine connection, we reasoned that replacing these aryl groups with Ph would provide a similar steric environment at the Co center (L^3). The ortho Me groups in L^1 were kept due to their steric impact, but the para Me was removed for computational efficiency; *i.e.* 2,6-dimethylphenyl was modeled instead of mesityl (L^4). Only half of each dinucleating complex was modeled: **1** as a neutral singlet dicobalt species with L^3 denoted **i**, **2b** as a neutral singlet dicobalt species with L_4 denoted **iib**, **3** as a cationic triplet monocobalt species with L^4 denoted **iii**, **4** as a cationic singlet monocobalt species with L^3 denoted **iv**, and **5** as a cationic singlet monocobalt species with L^4 denoted **v** (see Figure S50 for the schematic description of all models). We analyze these compounds in reverse order below due to their increasingly complicated electronic structures.

iv and **v** optimized to similar structures with Co–N bond lengths that all agreed within 0.01 Å, and deviated from the x-ray structure of **4** by at most 0.04 Å for the equitorial acetonitrile ligand (Table 2). Both **iv** and **v** show intraligand bond lengths of 1.32, 1.43, and 1.37 Å for the C_{im}–N_{im}, C_{im}–C_{pyr}, and C_{pyr}–N_{pyr} bond lengths, respectively, suggesting that the ligand is a radical anion. Visualization of the spin density for **iv** confirms this (see ESI for the spin

density of **v**), which implies the bis(acetonitrile) complex is best described as having a low-spin cobalt(II) ion ($^{LS}Co^{II}$) antiferromagnetically coupled to an anionic bis(imino)pyridine ligand radical. This assignment of $^{LS}Co^{II}$ is consistent with the short equitorial Co–N bonds and elongated Co–NCMe$_{ax}$ bond length.

Bond	4	iv	v
Co–NCMe$_{ax}$	2.030	2.000	2.003
Co–NCMe$_{eq}$	1.928	1.889	1.893
Co–N$_{pyr}$	1.814	1.833	1.833
Co–N$_{im}$	1.934	1.945	1.942
Co–N$_{im}$'	1.936	1.945	1.943

Table 2. Summary of selected bond lengths in **4**, **iv**, and **v** where pyr and im stand for pyridine and imine.
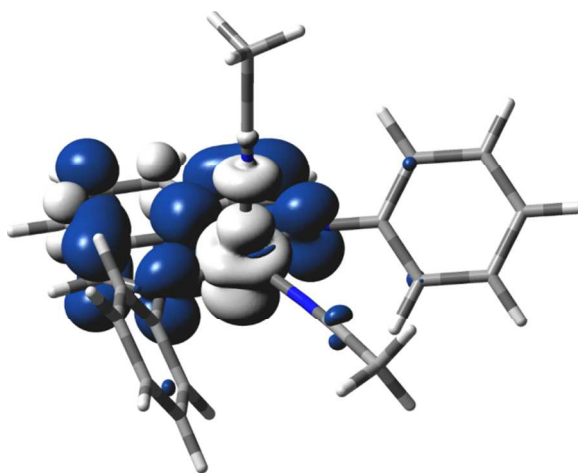

Figure 7. Spin density isosurface plot (iso = 0.002 au) for **iv**. Blue and white represent excess of α and β density.

iii was optimized as a cationic triplet due to the paramagnetic broadening observed in the ^{1}H NMR spectra of **3**. As Table 3 shows, however, the optimized Co–N bond lengths for this structure are inconsistent with the x-ray structure, especially Co–N$_4$ (one of the Co–N$_{im}$ bonds in the terdentate ligand) that is predicted to be too long by ~0.4 Å. This value far exceeds the typical structural error in DFT and, along with the asymmetric distortion of the Co–N$_{im}$ bonds in the tridentate ligand, suggests a high-spin electron configuration at the Co^{II} center. Thus, we also optimized **iii** as a singlet and much better structural agreement is observed with a maximum deviation of 0.03 Å in the Co–N$_{pyr}$ bond. This structure is predicted to be *higher* in free energy

than the triplet by 6.0 kcal/mol ($\Delta E(SCF)$ = 1.5 kcal/mol). It is important to note that our DFT modeling only considers the cation of the $[Co(L^2)_2][Co(CO)_4]$ ion pair. It is possible that intermolecular interactions cause the singlet to be lower in energy in the solid-state, whereas our modeling of $[Co(L^1)]^+$ by itself, which should more accurately represent the form in solution, predicts the triplet to be favored consistent with the experimentally observed paramagnetism. Both $\mathbf{iii}_{S=1}$ and $\mathbf{iii}_{S=0}$ are predicted to feature a monoanionic terdentate bis(imino)pyridine radical antiferromagnetically coupled to $^{HS}Co^{II}$ and $^{LS}Co^{II}$ ions, respectively, as shown by the spin density plots in Figure 8. The bidentate bis(imino)pyridine is predicted to be neutral in each structure, as evidenced by a lack of spin density on that ligand.

Bond	3	$\mathbf{iii}_{S=1}$	$\mathbf{iii}_{S=0}$
$Co-N_1$	2.012	2.050	1.992
$Co-N_2$	2.030	2.069	2.047
$Co-N_3$	1.945	2.084	1.944
$Co-N_4$	1.978	2.365	1.998
$Co-N_5$	1.810	1.928	1.838

Table 3. Summary of selected bond lengths in **3**, $\mathbf{iii}_{S=1}$, and $\mathbf{iii}_{S=0}$. N_1 and N_2 are in the bidentate ligand and N_3-N_5 are in the tridentate ligand, as shown in Figure 4.
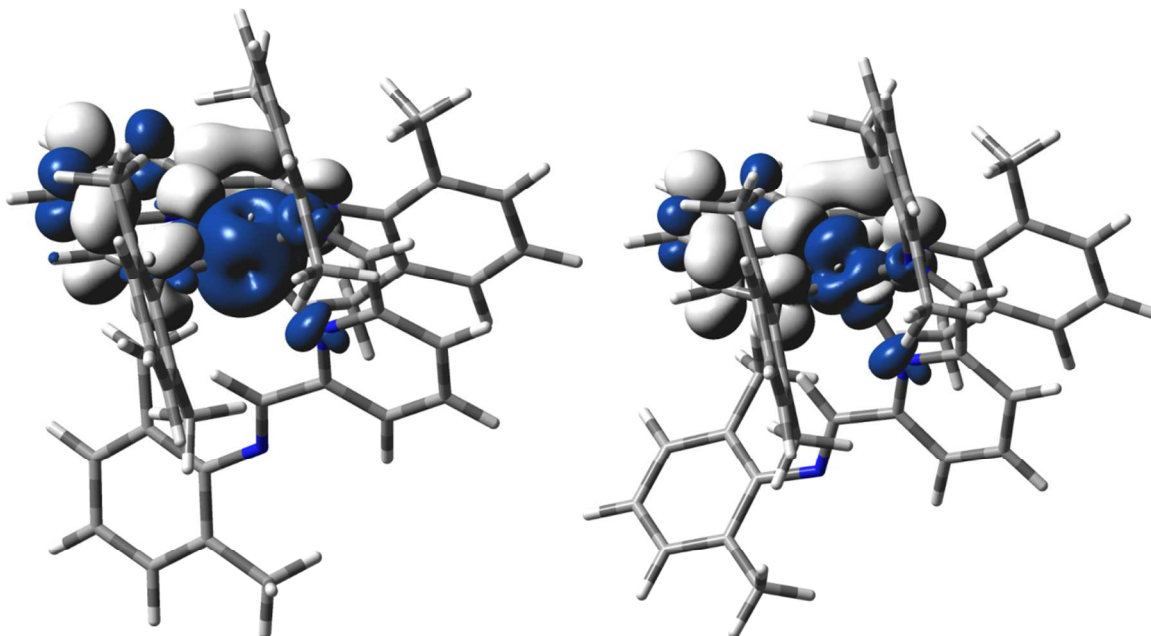

Figure 8. Spin density isosurface plots (iso = 0.002 au) for $\mathbf{iii}_{S=1}$ (left) and $\mathbf{iii}_{S=0}$ (right). Blue and white represent excess of α and β density.

i and **iib** were optimized as neutral species differing in the aryl substituents on the bis(imino)pyridine ligand. We were unable to reproduce the geometry of **2a** in these bimetallic model calculations. The crystallographic bond lengths of **1** are reproduced well by **i** ($\pm$ 0.02 Å) with the exception of the Co–Co distance that is ~0.1 Å too short (see Table S2). Intraligand bond lengths in **i** are 1.32, 1.43, and 1.37 Å for C_{im}–N_{im}, C_{im}–C_{pyr}, and C_{pyr}–N_{pyr}. Slightly larger discrepancies are seen between **2b** and **iib**, with deviations up to 0.04 Å except: (i) two of the bridging Co–carbonyl bonds have errors of 0.08 and 0.14 Å, and (ii) better agreement in the Co---Co interaction that is only 0.03 Å too short (see Table S3). Intraligand bond lengths in **iib** are 1.32, 1.42, and 1.37 Å for C_{im}–N_{im}, C_{im}–C_{pyr}, and C_{pyr}–N_{pyr}. These intraligand bond lengths, which are similar to those in **iv** and **v**, suggest that the bis(imino)pyridine ligand is a radical anion. However, closed-shell wavefunctions were found for both **i** and **iib** (after starting with open-shell, broken symmetry guess wavefunctions). To address the charges of the metal centers, the Natural Bonding Orbitals were generated to analyze the Natural Atomic Charges.[35] Co1 and Co2 (Co1 bound to L^3, see Figure 1) have charges of 0.42 and -0.50 in **i**, and Co3 and Co4 (Co3 bound to L^4, see Figure 3) have charges of 0.47 and -0.52 in **iib**; these values that differ by ~1 suggest that the cobalt bound to the iminopyridine is in a higher oxidation state than the one that is only bound to carbonyls. Given the neutral overall charge, and the anionic ligand charge inferred from the intraligand bond lengths, this would lead to assignment of the oxidation states as Co^I and Co^0, respectively. However, a Co^{-I} was inferred from the experimental carbonyl stretches. **i** is calculated to have a frequency at 1913 cm^{-1} that corresponds to stretching of the carbonyls on the $Co(CO)_4$ fragment.[36] **iib** is calculated to have frequencies at 1806 and 1845 cm^{-1} that correspond to the asymmetric and symmetric stretches of the bridging carbonyls, respectively, and the $Co(CO)_3$ fragment has stretches between 1978-2034 cm^{-1}. Thus, it seems reasonable that the observed stretch at 1802 cm^{-1} in **2** can be attributed to bridging carbonyls. However, the low frequency mode in **i** suggests formulation as Co^{II}/Co^{-I} instead, even though no evidence for spin polarization at the Co bound to the bis(imino)pyridine is observed. The Natural Atomic Charges are not capable of distinguishing between these valence limits (Co^I/Co^0 <-> Co^{II}/Co^{-1}) as they do not correspond to oxidation states.

Bridged and unbridged $Co_2(CO)_8$ have been studied extensively to determine what kind of theoretical analysis can determine the bonding (or lack thereof) between the metal centers.[37] Topological analyses were performed for the previously characterized $Co_2(CO)_8$ species, **i**, and

iib for a comparison at a common level of theory.[38] Table 4 summarizes these results. For $Co_2(CO)_8$, important differences of the bond critical point (bcp) between the bonded (unbridged) and unbonded (bridged) species include: (i) the nature of the bcp, (ii) lower density in the bonded species, (iii) much smaller Laplacian values for the bonded species, (iv) lower kinetic energy per electron ($G(r)/\rho$), and (v) a larger $|V(r)|/G(r)$ ratio.[37d] The bcp and electron density are similar for **i** and **iib**, but differences are observed in the other metrics. Whereas nearly an order of magnitude difference was observed for the Laplacian in $Co_2(CO)_8$, a difference of only 2-3 times (0.0525 vs. 0.129) is seen in **i** and **iib**. The kinetic energy per electron in both **i** and **iib** is larger than unbonded $Co_2(CO)_8$ but smaller than bonded $Co_2(CO)_8$, with an appreciable difference of ~0.3 for **i** and **iib** (vs. 0.6 for dicobalt octacarbonyl). Finally, the $|V(r)|/G(r)$ ratio that Gatti and Lasi recommended as a useful metric for distinguishing M–M bonded and non-bonded compounds does not approach the value of 2, even for unbridged $Co_2(CO)_8$, that they observed.[37d] However, the value of this ratio for **iib** is quite similar to bridged $Co_2(CO)_8$ (1.2 vs. 1.1), and the value for **i** of 1.3 is only slightly larger and much smaller than the value for unbridged $Co_2(CO)_8$ of 1.7. Collectively, we interpret these values to indicate that a cobalt-cobalt bond exists in **i** but not **iib**, however the difference in bonding is smaller than in $Co_2(CO)_8$. A source function analysis of these bond critical points also supports this interpretation and the difference in oxidation state between the Co centers (see ESI).[37d,39]

Species	bcp	ρ $(10^2$ au)	$\nabla^2\rho$ $(10^2$ au)	$G(r)$ $(10^2$ au)	$V(r)$ $(10^2$ au)	$G(r)/\rho$	$|V(r)|/G(r)$
unbridged $Co_2(CO)_8$	(3,−1)	3.84	1.69	1.25	8.28	0.33	1.7
bridged $Co_2(CO)_8$	(3,+1)	4.69	15.3	4.56	7.26	0.97	1.2
i	(3,−1)	3.23	5.25	1.77	4.63	0.55	1.3
iib	(3,+1)	4.30	12.9	3.68	4.60	0.86	1.1

Table 4. Topological properties at the bond critical point in bridged $Co_2(CO)_8$, unbridged $Co_2(CO)_8$, **i**, and **iib**. ρ is the electron density, $G(r)$ is the kinetic energy density, and $V(r)$ is the potential energy density.
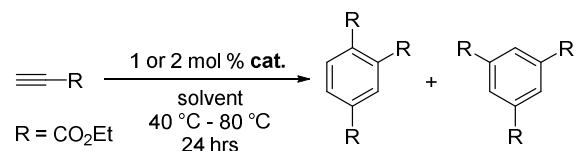
Reactivity of tetranuclear, dinuclear, and mononuclear cobalt complexes in alkyne cyclotrimerization

Having synthesized cobalt complexes **1-5**, we have conducted initial screening of their catalytic reactivity. We specifically focused on cyclotrimerization of ethyl propiolate, as (1)

$Co_2(CO)_8$ is known to catalyze alkyne cyclotrimerization;[40] (2) it was previously shown that bimetallic complexes exhibit cooperative reactivity in cyclotrimerizations;[41] (3) it is often considered a superior cyclotrimerization substrate compared with more electron-rich or bulkier substrates.[41] The results are summarized in **Table 5**. Reactions were carried out under three different sets of conditions: 40 °C in CD_2Cl_2, 80 °C in C_7D_8 (toluene-d_8), and 70 °C in CD_3CN. The reactivity studies reveal that while complexes **1-5** are competent cyclotrimerization catalysts, their reactivity is inferior to the reactivity of $Co_2(CO)_8$. At relatively low reaction temperature (40 ºC), complexes **1**, **2**, **4**, and **5** exhibit low, fairly similar conversion rates ranging between 20-28%. In contrast, $Co_2(CO)_8$ exhibits 60% conversion. It is also worth noting that complex **3** demonstrates the lowest reactivity at room temperature, consistent with the structure lacking vacant positions available for catalysis. At higher temperature (80 °C in toluene-d_8) all complexes exhibit similar reactivity (50-70% conversion), including complex **3**, likely indicating loss of one of the bis(imino)pyridines. Again, $Co_2(CO)_8$ is more reactive and exhibits nearly quantitative conversion at this temperature. Finally, we also tested the reactivity of acetonitrile adducts in this solvent. The reactivity of the $Co_2(CO)_8$ pre-catalyst was also tested in acetonitrile, although it is likely that $Co_2(CO)_8$ is also converted into a zwitterion in this solvent.[32, 33] In acetonitrile, all complexes exhibited low reactivity, including $Co_2(CO)_8$, likely due to the reaction inhibition by coordinating solvent.

While it is clear that complexes **3-5** demonstrate inferior reactivity compared with $Co_2(CO)_8$ due to the lack of available positions, it is less clear why complexes **1** and **2** are less reactive. One possible reason is the significantly increased steric bulk around the metal(s), compared with $Co_2(CO)_8$, which is detrimental to cyclotrimerization that requires several vacant positions. It is also possible, however, that while $Co_2(CO)_8$ exhibits a cooperative bimetallic effect in cyclotrimerization,[41b, 41c] complexes **1** and **2** disproportionate in solution into zwitterions and therefore catalyze this reaction in a monometallic fashion. Our future endeavors will focus on other catalytic applications of these systems.

Table 5. Reactivity of complexes 1-5 and $Co_2(CO)_8$ in cyclotrimerization of ethyl propiolate under three different sets of conditions.

Cat.	Solv, T	Mol%	% conv.	%1,2,4/ %1,3,5
1	CD_2Cl_2,	1	20	16 / 4
2	40 °C	2	28	16 / 12
4		1	21	14 / 9
5		2	24	14 / 10
3		2	12	6 / 6
$Co_2(CO)_8$		2	61	35 / 26
1	C_7D_8	1	66	38 / 28
2	80 °C	2	71	41 / 30
4		1	65	38 / 27
5		2	49	29 / 20
3		2	51	28 / 23
$Co_2(CO)_8$		2	99	63 / 36
4	CD_3CN	1	12	7/5
5	70 °C	2	16	7/9
$Co_2(CO)_8$		2	17	12/5

Summary and Conclusions

In summary, we have investigated the capability of $Co_2(CO)_8$ to serve as a direct metal precursor for the formally low oxidation state complexes of cobalt with redox-active mononucleating and dinucleating bis(imino)pyridine ligands. Formation of tetranuclear, dinuclear and mononuclear complexes was observed. Spectroscopic, structural, and computational studies revealed a variety of products including metal-metal bonded penta-coordinate complex, mono- and dicarbonyl bridged dimers, and mononuclear/dinuclear complexes in which cobalt centers are isolated and feature labile ligands (NCMe) coordinated to the metal. The species with interacting Co centers reported here show a similar trend to $Co_2(CO)_8$ with less Co-Co bonding as the number of bridging carbonyls increases, despite

shorter distances between the metals, even though different oxidation states are involved (i.e. no longer two d^9 centers). The complexes with a well-defined monometallic environment, even if it was embedded in a dinuclear complex, were best characterized as Co^{II} with a bis(iminopyridine) ligand radical. Species **1** and **2** exhibit intraligand bond lengths suggesting a ligand radical as well, however, neither the spectroscopy nor the calculations clearly point to a particular set of oxidation states ($Co^{I}/Co^{0} <-> Co^{II}/Co^{-I}$) for the metals. Overall, this work demonstrates promise of $Co_2(CO)_8$ in its capacity to serve as a precusor for multimetallic complexes with redox-active ligands.

†Electronic supplementary information (ESI) available: Synthetic procedures, experimental data, and Cartesian coordinates.

Acknowledgements

References

1. A. L. Gavrilova and B. Bosnich, *Chem. Rev.*, 2004, **104**, 349–383.

2. (a) N. Mankad, *Chem. Commun.*, 2018, **54**, 1291-1302. (b) I. G. Powers and C. Uyeda, *ACS Catalysis,* 2017, **7**, 936-958. (c) P. Buchwalter, J. Rosé and P. Braunstein*, Chem. Rev.*, 2015, **115**, 28−126. (d) J. F. Berry, *J. Chem. Sci.*, 2015, **127**, 209–214. (d) C. M. Thomas, *Comments Inorg. Chem.* 2011, **32**, 14-38. (f). R. M. Haak, S. J. Wezenberg and A. W. Kleij*, Chem. Commun.*, 2010, **46**, 2713–2723.

3. (a) F. Gloaguen and T. B. Rauchfuss, *Chem. Soc. Rev.*, 2009, **38**, 100–108. (b) S. C. Lee, W. Lo and R. H. Holm, *Chem. Rev.* 2014, **114**, 3579−3600. (c) S. Friedle, E. Reisner and S. J. Lippard, *Chem. Soc. Rev.*, 2010, **39**, 2768–2779.

4. For selected recent examples, see: (a) D.-H. Kwon, M. Proctor, S. Mendoza, C. Uyeda and D. H. Ess, *ACS Catal.*, 2017, 7, 4796-4804. (b) M. J. Behlen, Y.-Y. Zhou, T. J. Steiman, S. Pal, D. R. Hartline, M. Zeller and C. Uyeda, *Dalton Trans.*, 2017, **46**, 5493-5497. (c) K. T. Horak, A. Velian, M. W. Day and T. Agapie *Chem. Commun.*, 2014, **50**, 4427-4429. (d) D. L. J. Broere, D. K. Modder, E. Blokker, M. A. Siegler and J. I. van der Vlugt, *Angew. Chem. Int. Ed.*, 2016, **55**, 2406 –2410. (e) R. L. Hollingsworth, A. Bheemaraju, N. Lenca, R. L. Lord and S Groysman, *Dalton Trans.*, 2017, **46**, 5605-5616. (f) C. Camp, D. Toniolo, J. Andrez, J. Pécauta and M Mazzanti, *Dalton Trans.*, 2017, **46**, 11145–11148. (g) S. Suseno, K. T. Horak, M. W. Day and T. Agapie, *Organometallics*, 2013, **32**, 6883–6886. (h) S. Fortier, J. J. Le Roy, C.-H. Chen, V. Vieru, M. Murugesu, L. F. Chibotaru, D. J. Mindiola and K. G. Caulton, *J. Am. Chem. Soc.*, 2013, **135**, 14670–14678.

5. V. Lyaskovskyy and B. de Bruin, *ACS Catal.*, 2012, **2**, 270-279.

6. S. Enthaler, K. Junge and M. Beller, *Angew Chem Int Ed Engl.* 2008, **47**, 3317-3321.

7. K. G. Caulton, *Eur. J. Inorg. Chem.*, 2012, 435-443.

8. Q. Knijnenburg, S. Gambarotta and P H. M. Budzelaar, *Dalton Trans.*, 2006, 5442-5448.

9. For selected references, see: (a) S. Fortier, J. J. Le Roy, C.-H. Chen, V. Vieru, M. Murugesu, L. F. Chibotaru, D. J. Mindiola and K. G. Caulton, *J. Am. Chem. Soc.*, 2013, **135**, 14670–14678. (b) S. Fortier, O. González-del Moral, C.-H. Chen, M. Pink, J.J. Le Roy, M. Murugesu, D. J. Mindiola and K. G. Caulton, *Chem. Comm.* 2012, **48**, 11082-11084. (c) T. D. Manuel and J.-U. Rohde, *J. Am. Chem. Soc.,* 2009, **131**, 15582–15583. (d) B. R. Reed, S. A. Stoian, R. L. Lord, and S. Groysman, *Chem. Commun.*, 2015, **51**, 6496-6499. (e) D. Zhu, I. Thapa, I. Korobkov, S. Gambarotta and P. H. M. Budzelaar, *Inorg. Chem.*, 2011, **50**, 9879-9887. (f) T. W. Myers and L. A. Berben, *Chem. Commun.*, 2013, 49, 4175-4177. (f) S. C. Bart, K. Chlopek, E. Bill, M. W. Bouwkamp, E. Lobkovsky, F. Neese, K. Wieghardt and P. J. Chirik, *J. Am. Chem. Soc.*, 2006,

128, 13901-13912. (g) M. W. Bouwkamp, S. Bart, E. J. Hawrelak, R. J. Trovitch, E. Lobkovsky and P. J. Chirik, *Chem. Commun.*, 2005, 3406- 3408.

10. (a) S. C. Bart, E. Lobkovsky and P. J. Chirik, *J. Am. Chem. Soc.* 2004, **126**, 13794. (b) S. C. Bart, E. Lobkovsky, E. Bill, K. Wieghardt and P. J. Chirik, *Inorg. Chem.* 2007, **46**, 7055-7063. (c) A. M. Tondreau, C. Milsmann, E. Lobkovsky and P. J. Chirik, *Inorg. Chem.* 2011, **50**, 9888–9895.

11. L. Mond, C. Langer and F. Quincke, *J. Chem. Soc. Trans.* 1890, **57**, 749–753.

12. For selected examples, see: (a) C. C. Lu, E. Bill, T. Weyhermüller, E. Bothe and K. Wieghardt, *Inorg. Chem.* 2007, **46**, 7880−7889. (b) C. C. Lu, E. Bill, T. Weyhermüller, E. Bothe and K. Wieghardt, *J. Am. Chem. Soc.* 2008, **130**, 3181-3197. (c) A. Bheemaraju, J. W. Beattie, R. L. Lord, P. D. Martin and S. Groysman, *Chem. Commun.* 2012, **48**, 9595–9597. (d) A. Bheemaraju, J. W. Beattie, E. G. Tabasan, P. D. Martin, R. L. Lord and S. Groysman, *Organometallics*, 2013, **32**, 2952-2962. (e) A. Bheemaraju, R. L. Lord, P. Müller and S. Groysman, O*rganometallics* 2012, **31**, 2120-2123. (f) B. R. Reed, M. Yousif, R. L. Lord, M. McKinnon, J. Rochford and S. Groysman, *Organometallics*, 2017, **36**, 582-593.

13. (a) E. W. Abel and F. G. A. Stone, *Q. Rev. Chem. Soc.*, 1970, **24**, 498-552. (b) L. Mond, H. Hirtz and M. D. Cowa, *J. Chem. Soc. Trans.* 1910, **97**, 798

14. For selected recent examples, see: (a) G. G. Melikyan and B. Anker *Organometallics,* 2015, **34**, 4194−4197. (b) A. C. Coleman, C. Long, A. Meetsma, B. L. Feringa, W. R. Browne and M. T. Pryce, *Dalton Trans.*, 2009, 7885–7887. (c) T. León and E. Fernández, *Chem. Commun.*, 2016, **52**, 9363-9366. (d) R. Imayoshi, H. Tanaka, Y. Matsuo, M. Yuki, K. Nakajima, K. Yoshizawa and Y. Nishibayashi, *Chem. Eur. J.*, 2015, **21**, 8905–8909. (e) M. A. Henderson, J. Luo, A. Oliver and J. S. McIndoe, *Organometallics* 2011, **30**, 5471–5479. (f) S. Karabiyikoglu, B. A. Boon and C. A. Merlic, *J. Org. Chem.*, 2017, **82**, 7732−7744. (g) X. Creary, *J. Org. Chem.*, 2018, **83**, 136−144. (h) F. Hoffmann, J. Wagler and G. Roewer, *Organometallics,* 2014,

33, 5622−5625. (i) A. Dahan and M. Portnoy, *Chem. Commun.*, 2002, 0, 2700-2701. (j) Y. Li, J. A. Krause and H. Guan, *Organometallics,* 2018, **37**, 2147–2158.

15. For selected recent examples, see: (a) L. Wang, Z. Zeng, C. Ma, Y. Liu, M. Giroux, M. Chi, J. Jin, J. Greeley and C. Wang, *Nano Lett.,* 2017, **17**, 3391−3395. (b) C. Vollmer, R. Thomann and C. Janiak, *Dalton Trans.*, 2012, **41**, 9722–9727. (c) C.-Y. Kao, B. Li, Y. Lu, J.-W. Yoo and A. J. Epstein, *J. Mater. Chem. C*, 2014, **2**, 6171–6176. (d) Z. Wang, X. Hou, J. Shen and T. Li, *RSC Adv.*, 2016, **6**, 89503–89509. (e) J. A. Delgado, C. Claver, S. Castillón, D. Curulla-Ferré and C. Godard, *ACS Catal.*, 2015, **5**, 4568−4578.

16. (a) A. Franken, T. D. McGrath and F. G. A. Stone, *Dalton Trans.*, 2009, 7353–7355. (b) S. Wolf and C. Feldmann, *Dalton Trans.*, 2012, **41**, 8455–8459. (c) A. Franken, T. D. McGrath and F. G. A. Stone, *Organometallics* 2010, **29**, 2234–2247. (d) H. D. Park, M. Dincă and Y. Román-Leshkov, *ACS Cent. Sci.* 2017, **3**, 444−448.

17. (a) A. A. Zolotukhin, M. P. Bubnov, A. S. Bogomyakov, N. A. Protasenko, G. K. Fukin, I. D. Grishin and V. K. Cherkasov, *Inorg. Chim. Acta* 2016, **440**, 16–20. (b) A. L. Smith, L. A. Clapp, K. I. Hardcastle and J. D. Soper, *Polyhedron* 2010, **29**, 164–169. (c) N. A. Protasenko, A. I. Poddel'sky, A. S. Bogomyakov, G. K. Fukin and V. K. Cherkasov, *Inorg. Chem.* 2015, **54**, 6078−6080. (d) S. Bin-Salamon, S. H. Brewer, E. C. Depperman, S. Franzen, J. W. Kampf, M. L. Kirk, R. K. Kumar, S. Lappi, K. Peariso, K. E. Preuss and D. A. Shultz, *Inorg. Chem.* 2006, **45**, 4461-4467.

18. I. Wender, H. W. Sternberg and M. Orchin *J. Am. Chem. Soc.*, 1952, **74**, 1216–1219.

19. J. England, E. Bill, T. Weyhermüller, F. Neese, M. Atanasov and K. Wieghardt, *Inorg. Chem.*, 2015, **54**, 12002−12018.

20. A. C. Bowman, C. Milsmann, C. C. H. Atienza, E. Lobkovsky, K. Wieghardt and P. J. Chirik, *J. Am. Chem. Soc.*, 2010, **132**, 1676–1684.

21. (a) T. S. Hollingsworth, R. L. Hollingsworth, T. Rosen and S. Groysman, *RSC Adv*., 2017, **7**, 41819-41829. (b) T. S. Hollingsworth, R. L. Hollingsworth, R. L. Lord and S. Groysman, *Dalton Trans*., 2018,47, 10017-10024.

22. J. W. Beattie, D. J. SantaLucia, D. W. White, and S. Groysman, *Inorg. Chim. Acta*., 2017, **460**, 8-16.

23. S. Takano, Y. Takeuchi, D. Takeuchi and K. Osakada, *Chem. Lett*. 2014, **43**, 465–467.

24. T. Y. Garcia, J. C. Fettinger, M. M. Olmstead and A. L. Balch, *Chem. Commun*. 2009, 7143-7145.

25. A. W. Addison, N. T. Rao, J. Reedijk, J. van Rijn and G. C. Verschoor, *J. Chem. Soc., Dalton Trans*. 1984, 1349-1356.

26. (a) G. Winkhaus and G. Wilkinson, *J. Chem. Soc*. 1961, 602. (b) E. O. Fischer, P. Kuzel and H. P. Fritz, *Z. Naturforsch*., *B* 1961, 16b, 138. (c) J. Newman and A. R. Manning, *J. Chem. Soc., Dalton Trans*., 1973, 1593−1601.

27. H. Van Rensburg, R. P. Tooze, D. F. Foster and A. M. Z. Slawin, *Inorg. Chem*., 2004, **43**, 2468-2470.

28. K. T. Horak, A. Velian, M. W. Day and T. Agapie, *Chem. Commun*., 2014, **50**, 4427-4429.

29. H. Behrens and W. Z. Aquila, *Anorg. Allg. Chem*., 1967, **356**, 8−21.

30. G. G. Sumner, H. P. Klug and L. E. Alexander *Acta Cryst*., 1964, **17**, 732-742.

31. (a) R. L. Sweany and T. L. Brown, *Inorg. Chem*. 1977, **16**, 415 - 421. (b) G. Aullón and S. Alvarez, *Eur. J. Inorg. Chem*. 2001, 3031-3038.

32. For selected references, see: (a) F. Calderazzo, F. Masi and G. Pampaloni, *Inorg. Chim. Acta* 2009, **362**, 4291–4297. (b) W. Hieber and R. Wiesboeck, *Chem. Ber*. 1958, **91**, 1230-1234. (c) A. Sacco, *Gazz. Chim. Ital*., 1953, **83**, 632. (d) A. Sisak and L. Markó, *J. Organomet. Chem*., 1987, **330**, 201-206. (e) E. Fuhrmann, *Chemiker Zeitung* 1988, **112**, 295.

33. L. T. Mika, R. Tuba, I. Tóth, S. Pitter and I. T. Horváth, *Organometallics*, 2011, **30**, 4751–4764.

34. See ESI for full computational details: (a) S. H. Vosko, L. Wilk, and M. Nusair, *Can. J. Phys.*, 1980, **58**, 1200-1211. (b) C. Lee, W. Yang, and R. G. Parr, *Phys. Rev. B*, 1988, **37**, 785-789. (c) A. D. Becke, *Phys. Rev. A*, 1988, **38**, 3098-3100. (d) A. D. Becke, *J. Chem. Phys.*, 1993, **98**, 1372-1377. (e) P. J. Stephens, F. J. Devlin, C. F. Chabalowski, and M. J. Frisch, *J. Phys. Chem.*, 1994, **98**, 11623-11627. (f) S. Grimme, J. Antony, S. Ehrlich, and H. Krieg, *J. Chem. Phys.*, 2010, **132**, 154104. (g) S. Grimme, S. Ehrlich, and L. Goerigk, *J. Comp. Chem.*, 2011, **32**, 1456-1465.

35. NBO Version 3.1, E. D. Glendening, A. E. Reed, J. E. Carpenter, and F. Weinhold.

36. The value for B3LYP/6-31G(d) of 0.952 was used for the scaling factor. I. M. Alecu, J. Zheng, Y. Zhao, and D. G. Truhlar, *J. Chem. Theory Comput.*, 2010, **6**, 2872-2887.

37. (a) C. Bo, J.-P. Sarasa, and J.-M. Poblet, *J. Phys. Chem.*, 1993, **97**, 6362-6366. (b) P. Macchi and A. Sironi, *Coord. Chem. Rev.*, 2003, **238-239**, 383-412. (c) O. Kluge, M. Finger, and J. Reinhold, *Inorg. Chem.*, 2005, **44**, 6494-6496. (d) C. Gatti and D. Lasi, *Faraday Discuss.*, 2007, **135**, 55-78. (e) R. Ponec, G. Lendvay, and J. Chaves, *J. Comput. Chem.*, 2008, **29**, 1387-1398. (f) J. C. Green, M. L. H. Green, and G. Parkin, *Chem. Commun.*, 2012, **48**, 11481-11503. (g) D. Tiana, E. Francisco, P. Macchi, A. Sironi, and A. M. Pendás, *J. Phys. Chem. A*, 2015, **119**, 2153-2160.

38. (a) R. F. W. Bader, *Chem. Rev.*, 1991, **91**, 893-928. (b) T. Lu and F. Chen, *J. Comput. Chem.*, 2011, **33**, 580-592.

39. (a) R. F. W. Bader and C. Gatti, *Chem. Phys. Lett.*, 1998, **287**, 233-238. (b) C. Gatti, F. Cargnoni, and L. Bertini, *J. Comput. Chem.*, 2003, **24**, 422-436.

40. (a) W. Hübel and C. Hoogzand, *Chem. Ber.*, 1960, **93**, 103-115. (b) U. Krüerke and W. Hübel, *Chem. Ber.*, 1961, **94**, 2829-2856; (c) C. Hoogzand and W. Hübel, *Tetrahedron Lett.*, 1961, 637-643. (d) M. A. Bennett and P. B. Donaldson, *Inorg. Chem.*, 1978, **17**, 1995–2000.

41. (a) K. Yamamoto, H. Nagae, H. Tsurug and K. Mashima, *Dalton Trans.*, 2016, **45**, 17072-17081. (b) R. J. Baxter, G. R. Knox, P. L. Pauson and M. D. Spicer, *Organometallics*, 1999, **18**, 197. (c) R. J. Baxter, G. R. Knox, J. H. Moir, P. L. Pauson and M. D. Spicer, *Organometallics*, 1999, **18**, 206-214. (d) K. Yamamoto, H. Tsurugi and K. Mashima, *Organometallics*, 2016, **35**, 1573-1581. (e) H.-Z. Chen, S.-C. Liu, C.-H. Yen, J.-S. K. Yu, Y.-J. Shieh, T.-S. Kuo and Y.-C. Tsai, *Angew. Chem., Int. Ed.*, 2012, **51**, 10342. (f) S. Pal and C. Uyeda, *J. Am. Chem. Soc.*, 2015, **137**, 8042-8045.
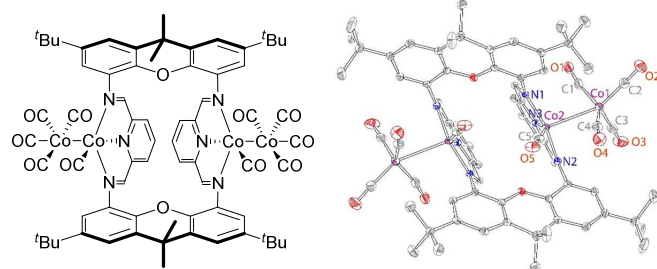
Reactivity of dicobalt octacarbonyl with dinucleating and mononucleating redox-active bis(imino)pyridines is investigated.